Spectrally asymmetric mode correlation and intensity noise in pump-noise-suppressed laser diodes

C. Becher,* E. Gehrig, and K.-J. Boller
Fachbereich Physik, Universität Kaiserslautern, Erwin Schrödinger Straße 46, 67663 Kaiserslautern, Germany
(Received 25 November 1997)

We report on the experimental observation of a spectrally asymmetric quantum correlation between the intensities of the main mode and a large number of weakly excited side modes in a pump-noise-suppressed laser diode. The total intensity noise of the laser diode results from a generally incomplete cancellation process between these mode intensities, which influences the generation of amplitude squeezed light. Nonlinear gain due to cross mode gain saturation in the semiconductor lasing medium is found to be the origin of the asymmetric intensity noise distribution between short- and long-wavelength side modes. The experimental results are in good agreement with the predictions of a multimode Langevin rate equation model including asymmetric nonlinear gain saturation. [S1050-2947(98)04605-8]

PACS number(s): 42.50.Dv, 42.50.Lc, 42.55.Px

I. INTRODUCTION

When the generation of amplitude squeezed light from diode lasers was theoretically predicted [1] and experimentally observed [2], it was considered to be a single-mode effect. Both the theoretical predictions and the experiments treated diode lasers featuring a single longitudinal mode spectrum. It was assumed that a pump-noise suppression by a high impedance constant current source, a high diode laser quantum efficiency, and a driving current high above threshold were sufficient requirements for the generation of amplitude squeezed light.

That picture of squeezed light generation turned out to be oversimplified. On the one hand, many diode lasers failed to produce amplitude squeezing even if they fulfilled the above requirements. Until now only a few types of diode lasers have shown the predicted behavior [3]. On the other hand, sub-shot-noise operation was found for a constant current driven semiconductor laser even though it was lasing on several longitudinal modes [4]. Spectrally resolved measurements revealed that the individual modes of that laser exhibited large excess noise above the standard quantum noise limit (SQL). It was shown that in the case of multimode oscillation, amplitude squeezing is due to a negative quantum correlation between the intensity fluctuations of the different longitudinal modes. The large intensity fluctuations of the individual modes then cancel to yield a total intensity noise that is suppressed to values below the SQL. Such perfect quantum correlation is formed only if the gain medium is nearly homogeneously broadened. The generation of amplitude squeezed light in multimode diode lasers, however, still requires the fulfillment of the above conditions of a high impedance constant current source, a high diode laser quantum efficiency, and a driving current high above threshold.

The consideration of multimode effects for the generation of amplitude squeezed light turned out to be essential also for so-called single-mode diode lasers, which generally exhibit a large number of weakly excited longitudinal side modes. The competition between these weak modes and the main mode for the total gain in the semiconductor medium gives rise to mode partition noise, which can lead to a large excess noise of the individual modes despite their low intensities. If the gain medium is not completely homogeneously broadened, the anticorrelation of the modes is degraded, the noise cancellation is not perfect, and thus the total intensity noise is increased. For that reason the total intensity noise depends very strongly on inhomogeneous gain contributions and subsequently on the degree of anticorrelation of the individual modes.

The influence of side mode power on the intensity noise was experimentally verified for squeezed light generation with injection-locked [5,6] and grating feedback laser diodes [7]. The generation [6,7] or enhancement [5] of squeezing in those experiments was explained by an increased suppression of the side mode intensity compared to the free-running case. In the free-running laser the negative intensity noise correlation was not perfect due to gain inhomogeneities, such that the mode partition noise was not completely suppressed and amplitude squeezing was degraded. The reduced side mode intensity in the case of injection-locking or grating feedback led to a reduction of the mode partition noise, while the imperfect negative correlation remained unchanged. Thus the total intensity noise was reduced due to the reduced contribution of the side modes. Recently, these results were confirmed by a detailed interferometric measurement of longitudinal mode partition noise in semiconductor lasers [8]. Similar effects of negative quantum correlations were also found for polarization modes in quantum-well diode lasers [9] and orthogonally polarized, transverse modes in microcavity lasers [10].

The dependence of longitudinal mode anticorrelation on gain inhomogeneities in ''quasi-single-mode'' diode lasers was studied recently [11]. It was shown that diode laser intensity noise and amplitude squeezing generally has to be considered a multimode effect and results from a cancellation among anticorrelated fluctuations of the main mode and

*Electronic address: cbecher@rhrk.uni-kl.de

all the weakly excited side modes. In addition to the studies above, it was found that not only the mode partition noise increases with increasing side mode power but also the mode anticorrelation decreases. This effect is due to an inhomogeneous self-saturation of each mode's gain by its own fluctuations, which adds up to the homogeneous gain saturation. Increasing side mode power thus leads to an increased inhomogeneity and subsequently to a reduced anticorrelation of the modes' fluctuations. The total intensity noise of the laser diode therefore depends critically on the amount of side mode suppression in the diode laser. These measurements revealed that only in the case of very high side mode suppression (>55 dB) diode laser amplitude squeezing can be considered to a good approximation a true single-mode effect.

In this paper we report on investigations on diode laser intensity noise that further extend the above picture of amplitude squeezing. We present detailed, spectrally resolved measurements of the intensity noise of a pump noise suppressed, single-mode quantum-well diode laser in three different configurations: free running, injection locked, and with external grating feedback. Our investigations reveal a strong asymmetry between the intensity noise of short- and long-wavelength side modes depending on the degree of side mode suppression. We show that amplitude squeezing in the injection-locked and grating feedback case results from a cancellation among the fluctuations of the main mode and more than 150 weakly excited side modes with asymmetric intensity and intensity noise distribution. Thus our results indicate that the anticorrelation of the side modes with the main mode is spectrally asymmetric.

We assume that this asymmetric correlation results from asymmetric nonlinear gain in the laser diode [12], which couples the fluctuations of the individual modes. The physical origin of the asymmetric nonlinear gain is a pulsation of the excited carrier population [13,14], induced by the beat of longitudinal modes, which modulates the total spectral gain distribution. Our results are in good agreement with the predictions of a multimode Langevin rate equation model [4] including gain inhomogeneities due to self-mode gain saturation by the fluctuations of each mode [11] and asymmetric cross-mode gain saturation [15]. This model also predicts the low-frequency intensity noise enhancement limiting the range of noise frequencies for which amplitude squeezing can be generated in diode lasers, as was experimentally observed recently [16]. The predictions of our model for the total diode laser intensity noise depend critically on the strength of the inhomogeneous contributions to the gain saturation and hence on the values of material parameters, such as relaxation times of the excited carriers. This critical dependence might explain why different types of diode lasers exhibit a completely different total intensity noise under the same external conditions, such as pump noise, pump level, and quantum efficiency, and why most of these diode lasers fail to produce amplitude squeezing even though the experimental requirements, as discussed above, are fulfilled.

II. EXPERIMENTAL RESULTS

In order to obtain detailed information on the dependence of the mode correlation on gain inhomogeneities in diode lasers and the contribution of the side modes to the total intensity noise we performed spectrally resolved intensity noise measurements. We investigated two single-mode, quantum-well diode lasers (SDL 5410-C) with emission wavelengths around 810 nm and output powers of 100 mW. The lasers were driven by a homebuilt high impedance constant current source to achieve pump noise suppression below the SQL. To examine the intensity noise in the different regimes of side mode suppression the lasers were operated in three different configurations: free running, injection locked (both laser 1), and with external grating feedback (laser 2). Injection locking was achieved with another grating stabilized diode laser used as the master laser. This system is described in detail elsewhere [16]. For the free-running and the injection-locked laser the threshold current was 19 mA and the operating current 115 mA.

The extended cavity setup was established by the feedback from a Littrow grating with 1200 l/mm placed at a 40 mm distance from the laser facet. The diffraction efficiency of the grating was 20% for the first order, which was fed back into the diode laser, and 68% for the zeroth order, which was used as output coupler. The laser threshold was 14 mA in this setup and the operating current 128 mA. Both investigated laser diodes featured a high quantum efficiency of 68%.

In order to determine the contribution of the individual side modes to the total intensity noise the diode laser radiation was passed through a homebuilt high transmission spectrometer that consisted of a grating with an efficiency of 66% in first order and an adjustable output slit. Both the position and the width of this output slit were variable such that the central transmission wavelength and the bandwidth could be chosen independently. Thus a variable number of modes out of the diode laser emission spectrum could be transmitted through the spectrometer. The intensity noise of the transmitted modes was measured on a single large area silicon p-i-n photodiode (Hamamatsu S3994, 93% quantum efficiency at 810 nm, 40-MHz cutoff frequency) placed behind the spectrometer. The photodiode signal was amplified by a rf amplifier (Miteq AU1310) and displayed on a rf spectrum analyzer (Advantest R3261A). We calibrated the SQL with the attenuated radiation of an array of light-emitting diodes generating the respective dc photocurrent. A minimum input power of 5 mW on the photodiode was required to achieve a signal current noise that exceeded the dark current noise of the photodiode by 6 dB, such that the contribution of the dark current to the total photodiode output could be neglected. As the side mode power was too weak to directly obtain this minimum signal current, the side modes were always detected together with the main mode. Thus, by adjusting the position and width of the output slit, the influence of a variable number of side modes on the total intensity noise could be investigated.

To control the resolution of the spectrometer the transmitted output was recorded with an optical spectrum analyzer (Ando AQ-6315A) with a resolution of 0.05 nm and a dynamic range of 70 dB. The resolution of the spectrometer was found to be better than 0.1 nm such that the longitudinal diode laser side modes with 0.11-nm spacing and roughly equal intensities could be resolved. For the free-running laser all modes could be separated from each other and for the

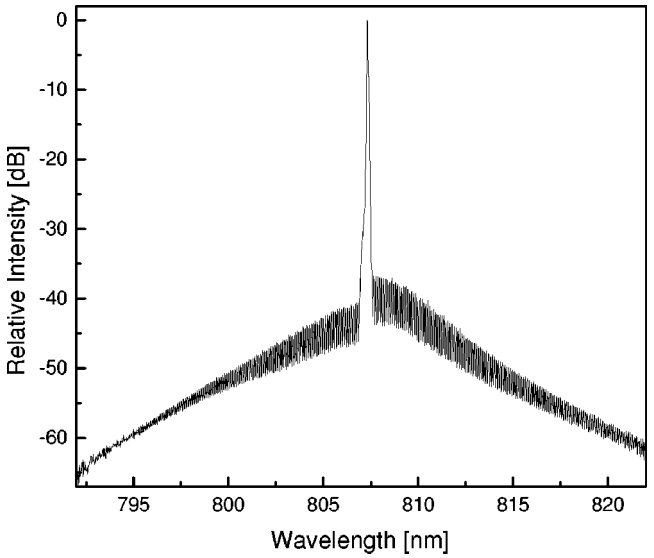

FIG. 1. Longitudinal mode spectrum of an injection-locked diode laser, recorded with an optical spectrum analyzer.

injection-locked laser all modes starting from the third mode adjacent to the main mode and starting from the fifth mode in the case of external feedback. This restriction in mode separation is due to the large intensity difference between the main mode and the adjacent side modes in the latter cases, reducing the spectrometer resolution. Nevertheless, an extrapolation of the number of transmitted modes dependent on the slit width allowed for a determination of the intensity noise of the main mode and the adjacent side modes to a good approximation. In all setups the diode lasers were isolated from the spectrometer and the detector by a 60-dB optical isolator (Gsänger DLI-1) to prevent any influence of back reflections on the diode laser spectrum and intensity noise.

Before the noise measurements were performed we recorded the diode laser emission spectra with the optical spectrum analyzer with the fiber input placed in front of the spectrometer. Figure 1 shows, for example, the spectrum of the injection locked diode laser over a wavelength range of 30 nm. The spectrum consists of the large peak of the main lasing mode and more than 250 weakly excited side modes. The intensity distribution of the side modes reveals a strong asymmetry between the short-wavelength (SW) and long-wavelength (LW) side modes, independent of the locking wavelength. The suppression of the maximum side mode intensity relative to the main mode in Fig. 1 is 37 dB for the LW side and 41 dB for the SW side, respectively. This side mode suppression (SMS) varied between 33 and 37 dB for the LW side modes and 37 and 41 dB for the SW side modes, depending on the injection-locking alignment. The asymmetric side mode distribution has been reported before [13,17] and was explained by asymmetric nonlinear gain due to a pulsation of the electron population at the beat frequency between longitudinal modes. We will show later that the asymmetric side mode distribution is predicted by a rate equation model including asymmetric nonlinear gain. The spectra for the free-running and the grating feedback diode laser revealed a similar asymmetric intensity distribution, but the difference in SMS is larger in the former case (around 5 dB) and smaller in the latter case (around 2 dB) compared to

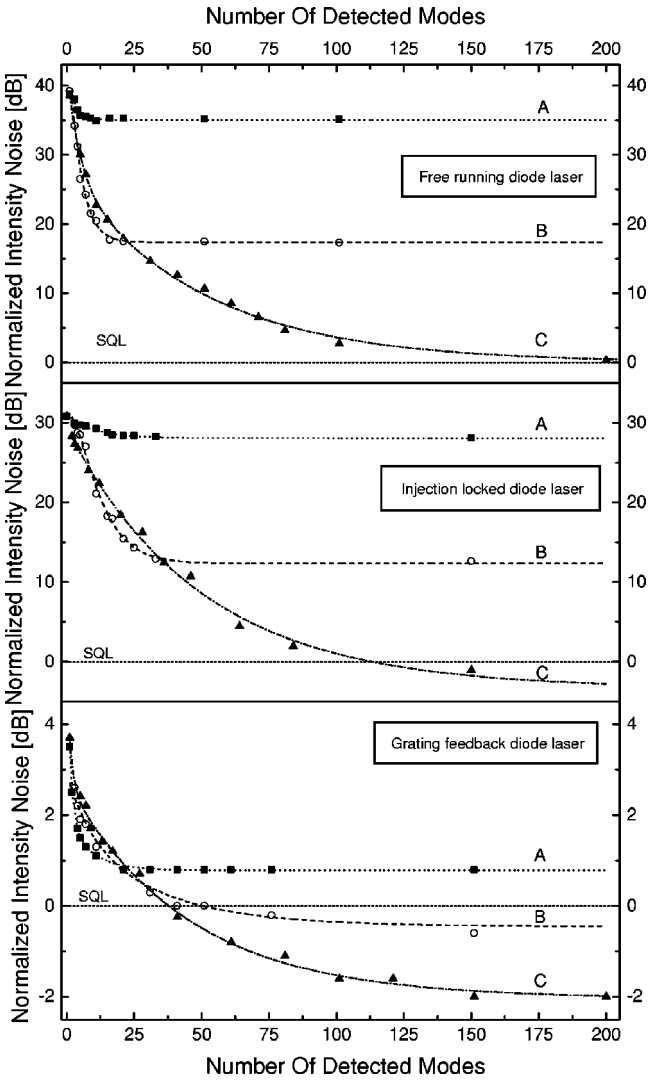

FIG. 2. Measured intensity noise at 30 MHz of a free-running, injection-locked, or grating feedback diode laser as a function of the number of detected side modes. Traces *A*, main mode with short-wavelength (SW) side modes; traces *B*, main mode with long-wavelength (LW) side modes; traces *C*, main mode with SW and LW side modes.

the injection-locked laser. In the case of the free-running laser the range of SMS was 22 and 29 dB for the LW and 27 and 34 dB for the SW modes, respectively, depending on the current through the laser diode, which shifts the emission wavelength and thus changes the emission spectrum. In the grating feedback laser the SMS varied between 45 and 55 dB for the LW and 47 and 57 dB for the SW modes, respectively, corresponding to the grade of feedback into the diode laser, which depended on the grating alignment.

In order to perform a spectrally resolved intensity noise measurement the spectrometer output slit was narrowed such that only the main mode was transmitted. Starting from that position, the slit was opened symmetrically around its center such that the main mode and an increasing number of side modes from both the SW and LW side successively were transmitted through the spectrometer and were detected on the photodiode. Traces *C* of Fig. 2 show the intensity noise measured at a noise frequency of 30 MHz for the different configurations. All intensity noise values are corrected for

the overall detection efficiency, which contains the photodiode quantum efficiency (93%), the spectrometer grating efficiency (66%), the transmission of the optical isolator (89%), and the feedback grating efficiency (68%) in the case of the extended cavity diode laser. In all configurations the main mode intensity noise was found to be well above the SQL: 38.6 dB for the free-running (FR) laser, 31.4 dB for the injection-locked (IL) laser, and 3.5 dB with the grating feedback (GF). When the slit was opened symmetrically around the main mode the intensity noise decreased exponentially with the number of additionally detected side modes, as is represented by the fit curves. This decrease is to values slightly above the SQL in the free-running case (0.3 dB). Amplitude squeezing of 1.3 dB was observed for the injection-locked laser only if more than 150 modes were transmitted simultaneously. In the grating feedback laser with a low SMS of 45 dB (LW modes) the intensity noise already dropped below the SQL with 50 detected modes, but the minimum value of 2.0 dB amplitude squeezing was reached in the limit of a high transmitted mode number only. The observed behavior clearly indicates that all the diode laser side modes contribute to the quantum anticorrelation with the main mode and to the cancellation process that determines the total intensity noise. Our results thus confirm the idea put forth in a previous study [11] that all the side modes should contribute, to some extent, to the cancellation effect. Even in the case of a very high SMS (55 dB) with the grating feedback laser the observed amplitude squeezing was found to result from a multimode cancellation. The main mode intensity noise in this case was measured to be at the SQL. However, if one additional side mode was detected together with the main mode, the resulting intensity noise was below the SQL. This again illustrates the nonclassical nature of the quantum anticorrelation between the different modes.

In addition to these results, our measurements show that the side mode contribution to the total intensity noise features a strong asymmetry. When the spectrometer output slit was opened asymmetrically such that the main mode was transmitted with an increasing number of either SW or LW side modes, respectively, the noise decrease was different for each case. If the main mode was detected together with the SW side modes, the noise decreased only moderately in all three configurations (traces *A* in Fig. 2): to 35.1 dB (FR), 28.7 dB (IL), and 0.8 dB (GF). A much higher reduction was observed when the LW side modes were detected in addition to the main mode (traces *B* in Fig. 2). For the free-running and the injection-locked laser the resulting noise levels of 17.3 and 13.1 dB, respectively, remained above the SQL. However, in the grating feedback laser amplitude squeezing of 0.5 dB is generated by the cancellation of main mode and LW side mode fluctuations. The difference in noise levels for the SW and LW sides of the diode laser spectrum proves that the quantum anticorrelation of the side modes with the main mode is spectrally asymmetric.

The range of noise frequencies for which amplitude squeezing can be obtained is limited towards low frequencies by an intensity noise enhancement. This low-frequency noise enhancement is present in the intensity noise spectra for all investigated setups. In Fig. 3 the intensity noise spectrum of the injection-locked diode laser, measured with a balanced homodyne detector [16], is displayed as an example. The total intensity noise rises above the SQL at a noise frequency of 2 MHz and reaches a value of 2.2 dB above the SQL at 100 kHz. This low-frequency noise enhancement is higher for the free-running laser (3.0 dB above the high-frequency noise floor) and much smaller for the grating feedback laser with 0.8 dB above the SQL for a SMS of 45 dB and 0.6 dB for a SMS of 55 dB. Thus the amount of low-frequency excess noise is found to be dependent on the SMS ratio. We will show that the origin of this excess noise is an incomplete cancellation of main mode and side mode fluctuations due to both symmetric and asymmetric gain inhomogeneities. The observation of low-frequency intensity noise has been reported previously [18] and was explained in terms of nonlinear asymmetric gain [15]. However, the importance of this effect for the generation of amplitude squeezed light has not been considered so far. In the following section we will show that all the above experimental observations are predicted by a Langevin rate equation model that considers gain inhomogeneities due to self-mode gain saturation and asymmetric cross-mode gain saturation.

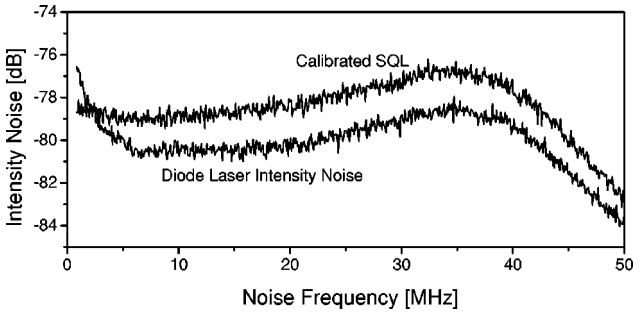

FIG. 3. Intensity noise spectrum of an injection-locked diode laser, measured with a balanced homodyne detector. Upper trace, calibrated SQL (homodyne difference signal); lower trace, diode laser intensity noise (homodyne sum signal).

III. THEORETICAL MODEL

An adequate model of diode laser intensity noise characteristics requires the consideration of nonlinear gain effects in the semiconductor lasing medium. This nonlinear gain arises due to spectral hole burning (self-saturation) by the lasing main mode and a pulsation of the electron population at the beat frequency between longitudinal modes (cross saturation) [19,20]. Both phenomena lead to an inhomogeneous saturation of the semiconductor laser's gain. The physical origin of the inhomogeneous contributions are the finite interband and intraband relaxation times, which limit the temporal response of the electron population to fluctuations of the internal laser field. In the case of cross-mode gain saturation these fluctuations emerge from the superposition of longitudinal modes, which modulate the internal field with a beat frequency corresponding to the mode spacing. Due to the finite relaxation times, the modulated field leads to a pulsation of the excited electron population, which in turn acts as a modulator generating sidebands in the spectral gain distribution. As these sidebands coincide with the longitudinal side mode frequencies, the gain of the respective side modes is modified. Thus each mode influences the gain experienced by all other modes, leading to a coupling of the

modes via the nonlinear gain. The strength of this mode coupling depends on the underlying physical mechanism. If the longitudinal mode spacing $\Delta\nu$ is smaller or comparable to the inverse of the electron spontaneous emission lifetime τ^{sp} (≈ 1 ns), the coupling is due to a modulation of the complete carrier density. If $\Delta\nu\tau^{sp} \gg 1$, due to a larger mode spacing, the excited carrier population cannot respond to the mode beating. In this case a nonlinear mode coupling can still be mediated by the finite intraband relaxation time (≈ 0.1 ps) and it is, however, weaker than in the first case. The asymmetry in the spectral gain distribution arises due to the band structure, i.e., the rapid change of the quasiequilibrium electron Fermi-Dirac distribution as a function of carrier density [20].

For a description of the diode laser dynamics we start from a multimode Langevin rate equation model with homogeneous gain distribution [4]. The mode spectrum of the quasi-single-mode diode laser is represented in our model by three modes: one main mode M_0 and two side modes, M_{-1} representing the short-wavelength side modes and M_1 representing the long-wavelength side modes, respectively. The inhomogeneous contributions to the gain are accounted for by two different terms. One represents cross-mode gain saturation, which couples the photon numbers of each mode [15] and thus also the fluctuations of each mode. This term has to contain both symmetric and asymmetric contributions [12,17,19,21]. The second term describes a self-saturation of each mode by its own fluctuations, as in [11]. Both terms are found to be necessary for an adequate description of the diode laser intensity noise characteristics. The equations for the photon numbers $n_i(t)$ of each mode M_i and the total number of excited carriers $N_c(t)$ are

$$\frac{dn_i(t)}{dt} = \left[g_i^L(t) - g_i^{NL}(t) - \frac{1}{\tau_i^c} \right] n_i(t) + g_i^L(t) + S_i(t) + G_i(t) + g_i(t) + f_i(t), \tag{1}$$

$$\frac{dN_c(t)}{dt} = P - \frac{N_c(t)}{\tau^{sp}} - \sum_i \{[g_i^L(t) - g_i^{NL}(t)] n_i(t) + g_i^L(t)\} + \Gamma_p(t) + \Gamma_{sp}(t) + \Gamma(t). \tag{2}$$

Here we have used the same notation as in [11]. The terms $g_i^L(t)$ and $g_i^{NL}(t)$ are the linear and nonlinear gain, respectively, given by

$$g_i^L(t) = \frac{\beta_i}{\tau^{sp}} N_c(t), \tag{3}$$

$$g_i^{NL}(t) = \sum_j \varepsilon_{ij} g_j^L(t) n_j(t). \tag{4}$$

The exact form of the nonlinear coupling factor ε_{ij} in Eq. (4) is given by [15,19]

$$\varepsilon_{ij} = \frac{\mu^2 \omega_0}{2\varepsilon_0 n\, n_g \hbar \overline{\gamma_c \gamma}} \frac{C_{ij}}{C_j} \frac{1 + \alpha\tau(\omega_i - \omega_j)}{1 + [\tau(\omega_i - \omega_j)]^2}. \tag{5}$$

The following parameters are used. β_i denotes the spontaneous emission factor into the corresponding mode. The relative gain of the side modes compared to the main mode, due to the finite gain bandwidth, is accounted for by a parameter m: $\beta_{-1,1} = m\ \beta_0$. Thus this relative gain parameter m determines the ratio of the main and side mode intensities for a free-running laser. The electron lifetime due to spontaneous emission is denoted by τ^{sp}. The photon decay rate of each mode is given by $1/\tau_i^c = 1/\tau^{pe} + 1/\tau_i^{po}$, where τ^{pe} is the decay time due to output coupling losses, which is assumed to be equal for all modes, and $\tau_{-1,1}^{po} = p\ \tau_0^{po}$ is the decay time due to internal losses.

The loss parameter p is defined as the ratio of the main mode to the side mode internal loss rate as in [11]. Decreasing values of p thereby correspond to a decrease in the side mode power. The loss parameter is introduced phenomenologically to allow for the simulation of the process of a main mode selection with a specific side mode suppression ratio in the different experimental setups in a unified approach. Physically, this mode selection process is accomplished differently in the different setups. In the free-running laser one would expect a value of $p = 1$ and the main mode is selected by the relative spectral position of the gain profile and the cavity mode resonances. Experimentally, however, it is observed that the SMS ratio varies with the driving current and the temperature because gain profile and cavity resonances feature a different spectral shift with varying current and temperature. In the injection-locked diode laser a specific SMS is achieved because the main mode experiences a higher net gain than other modes due to the additional power injected into the main mode from the master laser. The SMS ratio is determined by the injected master laser power. In the grating feedback case the mode selection and side mode suppression process is accomplished by the frequency-filtered back reflection of the external grating: The main mode that is reflected back into the cavity experiences lower losses than the other modes, which are not well reflected back into the cavity. In summary, one can describe the increasing SMS ratio by an increase of side mode losses in the free-running laser, by a decrease of main mode losses in the grating feedback laser, and by increasing injection of master laser power in the injection-locked laser. We numerically simulated these different mode selection processes in different rate equation models alternatively by increasing side mode losses (via the loss parameter p), decreasing main mode losses (by keeping $\tau_{-1,1}^{po}$ constant and varying τ_0^{po}), and by injecting additional photons into the main mode while keeping all mode losses constant. These calculations proved to reveal identical results for all three procedures provided, e.g., a particular value of the loss parameter p is considered equivalent to a particular choice of the injected master laser power. As a consequence, we chose to simulate the different setups within only one set of rate equations (1)–(5) and rather vary solely the loss parameter p to describe the experimentally observed SMS. For specific values of p the corresponding equivalent values of injected power are given in Sec. IV.

The self-saturation term $S_i(t)$ is defined as in [11]: $\tau_i^c S_i(t) = -s_i(t)[\langle n_i\rangle / P\tau_i^c]\delta n_i(t)$, with a self-saturation parameter s_i, the pumping rate P, and the photon number fluctuation $\delta n_i(t) = n_i(t) - \langle n_i\rangle$ around the mean values $\langle n_i\rangle$.

The terms $G_i(t)$, $g_i(t)$, and $f_i(t)$ are the Langevin noise terms due to stimulated emission, internal losses, and output coupling, respectively. Correspondingly, $\Gamma_p(t)$, $\Gamma_{sp}(t)$, and $\Gamma(t)$ are the Langevin noise terms for pump noise, spontaneous emission noise, and stimulated emission noise, respectively. The correlation functions for the Langevin terms are defined in [4]. The first term in the expression (5) for the nonlinear coupling factor ε_{ij}, determining the strength of the nonlinearity, contains the transition dipole moment μ, the mode lasing frequencies ω_i, the refractive index n, and the group index n_g. The intraband carrier relaxation rate γ_c is defined as $\gamma_c = \gamma_c\gamma_v/(\gamma_c+\gamma_v)$, with the intraband energy relaxation rates for the conduction and valence bands, γ_c and γ_v, respectively, which are the inverses of the corresponding relaxation times τ_c and τ_v. The polarization relaxation rate is $\gamma = 1/\tau_{in}$, with the polarization relaxation time τ_{in}. The factor C_{ij}/C_j accounts for a spatial mode overlap factor, which we set approximately equal to 1 for the longitudinal modes in the diode laser waveguide, thereby neglecting spatial inhomogeneities. There exists some controversy [19] about the correct values for the parameters α and τ in Eq. (5). From a comparison of our experimental results with the predictions of our model, we find that we have to identify α with the linewidth enhancement factor and τ with the polarization relaxation time τ_{in} to obtain a realistic magnitude for the nonlinearity. Thus the experimentally observed asymmetric nonlinear gain has to arise from a pulsation of the excited electron population rather than from intraband effects.

For our calculations we used the following numerical parameter values, which have been used elsewhere to model $Al_xGa_{1-x}As$ diode lasers (the corresponding references are given): $\beta_0 = 2.7\times10^{-6}$ [11], $\tau^{sp} = 5\times10^{-9}$ s, $\tau_c = \tau_v = 5\times10^{-14}$ s [22], $\tau_{in} = 1.2\times10^{-13}$ s (τ_{in} can change within one order of magnitude depending on the wavelength and electron density; see [23]), $\mu = 4.8\times10^{-29}$ C m, [24], $n = 3.6$, $n_g = 4$, and $\alpha = 3$ [19]. Typical values for the facet reflectivity of the SDL 5410-C diode laser are 3–6%. Correspondingly, the decay time due to output coupling was chosen $\tau^{pe} = 7\times10^{-12}$ s. In order to obtain the experimentally observed quantum efficiency of 68%, we assumed a decay time due to internal losses of $\tau_0^{po} = 1.5\times10^{-11}$ s. The pumping rate $r = I_{pump}/I_{th}$ was set to the values used in the experiments for the free-running and injection-locked laser ($r = 6$) or the grating feedback laser ($r = 9$). A value of the self-saturation parameter $s_i = 0.01$ led to theoretical predictions that agreed best with the experimentally observed intensity noise.

IV. THEORETICAL RESULTS

Before we used the theoretical model to simulate the diode laser intensity noise characteristics we first calculated the average values for the photon number by neglecting the Langevin noise terms in Eqs. (1) and (2) and setting the time derivatives to zero. The relative gain parameter m was chosen such that the resulting photon numbers agree with the experimentally observed values. Figure 4 shows the calculated mean photon numbers and the side mode suppression of both the side modes vs the loss parameter $\log_{10}(1-p)$ for $r = 6$ and $m = 0.9997$, corresponding to the cases of the free-running and injection-locked diode lasers. The main mode

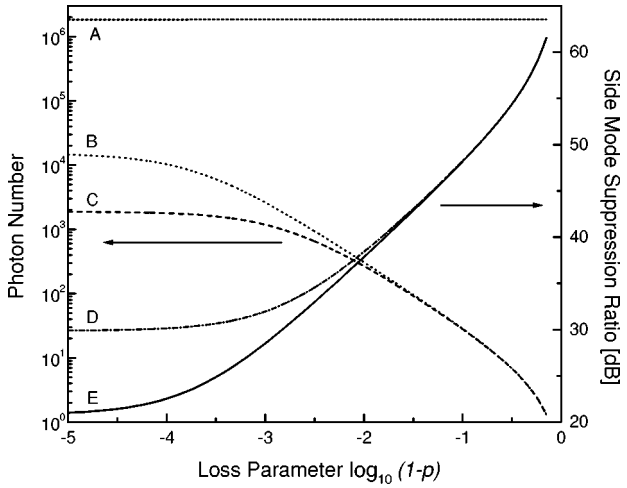

FIG. 4. Average photon numbers of the main and two (SW and LW) side modes, calculated as a function of the side mode loss parameter, for the free-running and the injection-locked diode laser. Also shown is the side mode suppression (SMS) ratio. Trace *A*, photon number of the main mode; trace *B*, photon number of the LW side mode; trace *C*, photon number of the SW side mode; trace *D*, SMS of the SW side mode; trace *E*, SMS of the LW side mode. The parameters are $r = 6$ and $m = 0.9997$. All other values are given in the text.

photon number (trace *A*) remains constant for all values of p, whereas the side mode photon numbers (traces *B* and *C*) decrease with increasing side mode losses. Our model predicts very well the asymmetric intensity distribution for the SW and LW side modes and the values for the SMS (traces *D* and *E*) that were measured for the free-running and injection-locked lasers. By a comparison of the SMS values in Fig. 4 with the experimentally obtained SMS ratios, one can identify the corresponding values of $\log_{10}(1-p)$, which are less than -3.5 (FR) and -3.5 to -2 (IL), respectively. In our simulation the values of $\log_{10}(1-p) = -3.5$ to -2 for the injection-locked laser yield the same SMS as the injection of 15–500 μW of master laser light into the diode laser cavity, respectively. The experimentally measured master laser power of 1 mW in front of the slave laser collimating lens [16] is in good agreement with those predicted values if one considers the imperfect mode matching of master and slave laser radiation. A calculation of the SMS for the grating feedback laser with parameters $r = 9$, $m = 0.9996$, and $\log_{10}(1-p) > -2$ reveals qualitatively similar results to those in Fig. 4, but the theoretically obtained difference in the SMS of the SW and the LW side modes (a 0.5-dB difference for a SMS of 45 dB and a 0-dB difference for a SMS of 55 dB) is too small compared to the experiment (approximately a 2-dB difference). From this we conclude that in the case of grating feedback one has to consider a stronger nonlinearity that is not accounted for by the above values of the parameters that contribute to the nonlinear coupling factor. This stronger nonlinearity arises due to the fact that in the presence of an external resonator the diode laser spectrum consists of the diode laser longitudinal modes, with a mode spacing of approximately equal to 50 GHz, superimposed by the modes of the external resonator, which have a much smaller spacing (approximately equal to 4 GHz). The excited electron population can react to the mode beating with the

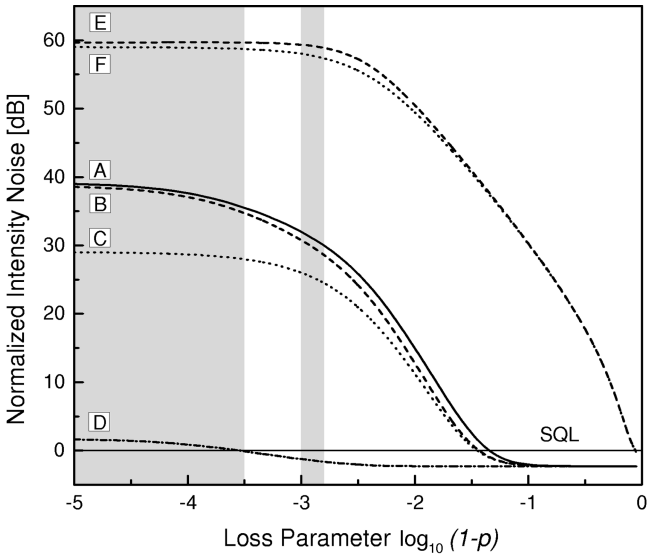

FIG. 5. Intensity noise at 30 MHz for various mode combinations of the free-running and injection-locked diode laser, calculated as a function of the side mode loss parameter. Trace *A*, main mode only; trace *B*, main mode with the SW side mode; trace *C*, main mode with the LW side mode; trace *D*, total diode laser intensity; trace *E*, LW side mode; trace *F*, SW side mode. The parameters are $r=6$ and $m=0.9997$. All other values are given in the text. The shaded regions indicate the side mode loss parameter ranges for the free-running and the injection-locked diode laser, respectively.

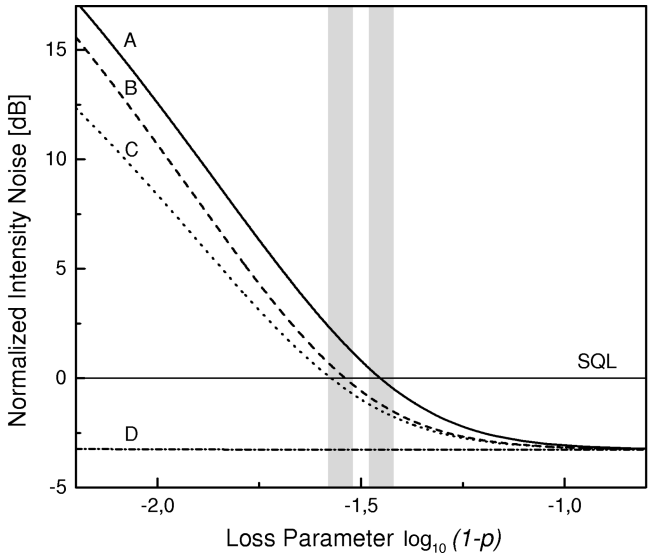

FIG. 6. Intensity noise at 30 MHz for various mode combinations of the grating feedback diode laser, calculated as a function of the side mode loss parameter. Trace *A*, main mode only; trace *B*, main mode with the SW side mode; trace *C*, main mode with the LW side mode; trace *D*, total diode laser intensity. The parameters are $r=9$ and $m=0.9996$. All other values are given in the text. The shaded regions indicate the side mode loss parameter ranges for the grating feedback diode laser with different SMS ratios, as discussed in the text.

time constant of the relaxation oscillation frequency approximately equal to 2.5 GHz. Thus the nonlinearity is much stronger for a beat frequency due to external cavity modes than for the beat frequency due to diode laser longitudinal modes.

With the calculated mean photon numbers one can now obtain the frequency-dependent intensity noise spectra for the individual modes and arbitrary mode combinations. For that purpose the standard linearization and Fourier transform procedure [4] is performed. Figure 5 displays the intensity noise, calculated for different combinations of simultaneously detected modes at a noise frequency of 30 MHz, vs the loss parameter p, for the case of the free-running and the injection-locked laser ($r=6$ and $m=0.9997$). The noise levels are each normalized to the respective SQL, employing the accompanying average photon number of each mode. The asymmetric intensity noise characteristics experimentally determined for the free-running and the injection-locked laser are well reproduced for values of $\log_{10}(1-p)$ of less than -3.5 (FR) and approximately equal to -2.9 (IL), respectively, indicated by the shaded regions in Fig. 5. In both cases the main mode intensity noise (trace *A*) is well above the SQL. The noise level of the main mode detected together with the SW side mode (trace *B*) is slightly lower and the main mode plus the LW side mode noise (trace *C*) is evidently lower than the noise of the main mode only. The side mode intensities (traces *E* and *F*) exhibit very large fluctuations despite their low photon numbers. The total intensity noise (trace *D*) is much lower due to the anticorrelation between the main mode fluctuations and the side mode fluctuations. It depends strongly on the value of p and is slightly above the SQL for the free-running laser and squeezed for the injection-locked laser. The exact value of this total intensity noise is found to depend strongly on the values of the self-saturation parameter s_i and the strength of the cross-mode gain saturation parameter ε_{ij}. These parameters, on the other hand, are subject to material parameters of the semiconductor lasing medium, such as carrier-carrier and carrier-phonon scattering times, which influence the typical relaxation times. We note that the contribution of both the self-saturation and the cross-mode gain saturation to the nonlinear gain are necessary to predict the experimentally obtained total intensity noise and asymmetry. This clearly indicates that the total intensity noise depends strongly on the inhomogeneous contributions to the gain saturation in the diode laser, which change the asymmetric mode anticorrelation and in turn depend on the ratio of the side mode suppression.

The range in Fig. 5 with values of $\log_{10}(1-p)>-2$ would in fact represent a grating feedback laser with a pump rate of $r=6$. For a comparison of the experimentally measured noise values with the predicted asymmetric intensity noise characteristics of the investigated grating feedback diode laser, Fig. 6 shows a detailed diagram, calculated with $r=9$ and $m=0.9996$. The experimentally observed SMS ratios of 45 and 55 dB are reproduced for values of $\log_{10}(1-p)=-1.55$ and -1.45, respectively, indicated by the shaded regions in Fig. 6. In our simulation the values of $\log_{10}(1-p)=-1.55$ to -1.45 correspond to a back reflection of 1.5–2.0 mW from the external grating into the diode laser cavity. From the measured free running power and the known grating efficiency we estimate that the reflected power from the grating was approximately 20 mW in front of the collimating lens. The theoretical and experimental values are in reasonable agreement if the imperfect coupling of

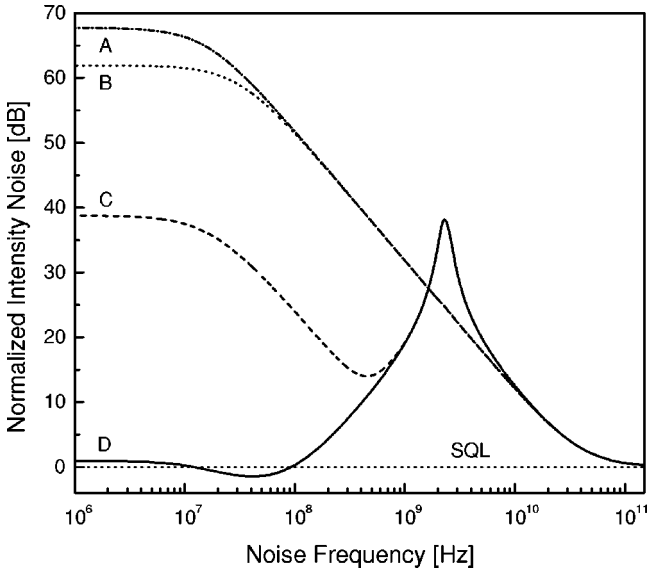

FIG. 7. Intensity noise spectra of the injection-locked diode laser, calculated as a function of the noise frequency. Trace *A*, long-wavelength side mode; trace *B*, short-wavelength side mode; trace *C*, main mode; trace *D*, total diode laser intensity. The parameters are $r=6$, $m=0.9997$, and $\log_{10}(1-p)=-2.9$. All other values are given in the text.

back-reflected light into the active region of the diode laser is considered, such as caused by uncompensated astigmatism and back reflection under a slight angle. In both cases the total intensity noise (trace *D*) is well below the SQL due to the strong mode anticorrelation, which in turn is subject to the high SMS. In the first case the asymmetric intensity noise values of Fig. 2 for the grating feedback laser are clearly predicted. The main mode intensity noise (trace *A*) is a few decibels above the SQL, the main mode plus the SW side mode noise (trace *B*) is only slightly above the SQL, and the main mode plus the LW side mode noise (trace *C*) exhibits a modest squeezing. In the second case the main mode intensity noise is at the SQL, whereas any other combination of detected modes shows amplitude squeezing. This again is in good agreement with the experimental observations. For the case of the grating feedback laser, single-mode squeezing should be obtainable for values of $\log_{10}(1-p)\gtrsim-1.4$, as was reported previously [11]. We note, however, that the exact value of the main mode noise depends strongly on the strength of the gain nonlinearity and might be different for the various types of diode lasers.

Our model can also predict the above-reported low-frequency intensity noise enhancement (see Fig. 3), limiting the range of noise frequencies for which amplitude squeezing can be generated. Figure 7 shows the calculated noise spectra for different modes and the total intensity of the injection-locked laser, calculated with the parameters $r=6$, $m=0.9997$, and $\log_{10}(1-p)=-2.9$. The LW and SW side modes (traces *A*and *B*) exhibit a very large intensity noise at low frequencies that rapidly decreases towards higher frequencies. This low-frequency side mode noise is due to the relaxation oscillations of the weakly excited side modes. Because of the weak excitation of the side modes, their relaxation oscillations occur at low frequencies. The strength of the relaxation oscillations damps out strongly with increasing frequency because the damping is enhanced by the nonlinear gain [15]. Due to the anticorrelation of the main mode with the side modes, the main mode intensity noise (trace *C*) also shows a large low-frequency enhancement, falling off towards higher frequencies and rising again at the main mode relaxation oscillation frequency of 2.5 GHz. The model predicts correctly the amplitude squeezing of the total intensity (trace *D*) for noise frequencies from 10 to 100 MHz and also the increase of the total intensity noise towards lower frequencies to values slightly above the SQL, as was found experimentally (compare to Fig. 3). This increase is caused by an imperfect anticorrelation of the side modes and the main mode due to the above-discussed gain inhomogeneities. A perfectly homogeneous broadened gain medium would exhibit amplitude squeezing over the complete frequency range below the relaxation oscillation resonance, as can be simulated with the theoretical model for values of $s_i=0$ and $\varepsilon_{ij}=0$. The strength of the low-frequency noise enhancement again depends largely on the strength of the self-mode and cross-mode gain saturation and may vary between different diode lasers. We note once more that both contributions to the nonlinear gain are necessary to predict the experimentally obtained total intensity noise and asymmetry.

V. CONCLUSIONS

We have presented spectrally resolved measurements of the intensity noise of pump-noise-suppressed, single-mode quantum-well diode lasers in different configurations. The results revealed a strong asymmetry between the intensity noise of the weakly excited short- and long-wavelength side modes and their contribution to the total diode laser intensity noise. Thus our investigations show that the anticorrelation of the side modes with the main mode is spectrally asymmetric. Our experimental results are in good agreement with the predictions of a three-mode Langevin rate equation model including gain inhomogeneities due to self-mode gain saturation and cross-mode gain saturation. In particular, we find that asymmetric nonlinear gain is the origin of the experimentally observed asymmetry of the mode anticorrelation. The diode laser total intensity noise depends strongly on the inhomogeneous contributions to the gain saturation, which change the asymmetric mode anticorrelation and in turn depend on the ratio of the side mode suppression. The total intensity noise and the low-frequency intensity noise enhancement, which limits the range of noise frequencies for which amplitude squeezing is obtainable, result from an imperfect cancellation among the main and side mode fluctuations and are reproduced correctly by the model. The predictions of our model for the absolute value of the total intensity noise, for the possibility to generate single-mode squeezing, and for the low-frequency intensity noise enhancement depend critically on the strength of the self-mode and cross-mode gain saturation. Since these contributions are subject to material properties of the semiconductor lasing medium, such as relaxation times, they should change considerably for different types of diode lasers. This critical dependence could thus explain why different diode lasers exhibit a completely different intensity noise characteristic and why some of them fail to produce amplitude squeezing even though the experimental requirements for that are fulfilled. The investi-

gation and the modeling of asymmetric effects in diode laser intensity noise may thus contribute to the understanding of the generation of amplitude squeezed light with diode lasers. Additionally, a systematic study of the dependence of diode laser intensity noise characteristics on semiconductor material properties, such as relaxation times, could lead to the establishment of design criteria for diode lasers that enable a reliable generation of single-mode squeezed light. This single-mode squeezed light is essential for experiments such as high-sensitivity spectroscopy [25,26] or the investigation of quantum noise properties of diode pumped solid-state lasers [16] and diode pumped continuous-wave optical parametric oscillators [27].

ACKNOWLEDGMENTS

The authors gratefully acknowledge the continuous support by Professor R. Wallenstein. This work was supported by the Deutsche Forschungsgemeinschaft.

[1] Y. Yamamoto and S. Machida, Phys. Rev. A **35**, 5114 (1987).
[2] S. Machida, Y. Yamamoto, and Y. Itaya, Phys. Rev. Lett. **58**, 1000 (1987).
[3] D. C. Kilper, M. J. Freeman, D. G. Steel, R. Craig, and D. R. Scifres, Proc. SPIE **2378**, 64 (1995).
[4] S. Inoue, H. Ohzu, S. Machida, and Y. Yamamoto, Phys. Rev. A **46**, 2757 (1992).
[5] S. Inoue, S. Machida, and Y. Yamamoto, Phys. Rev. A **48**, 2230 (1993).
[6] H. Wang, M. J. Freeman, and D. G. Steel, Phys. Rev. Lett. **71**, 3951 (1993).
[7] M. J. Freeman, H. Wang, D. G. Steel, R. Craig, and D. R. Scifres, Opt. Lett. **18**, 2141 (1993).
[8] S. Inoue, S. Lathi, and Y. Yamamoto, J. Opt. Soc. Am. B **14**, 2761 (1997).
[9] D. C. Kilper, D. G. Steel, R. Craig, and D. R. Scifres, Opt. Lett. **21**, 1283 (1996).
[10] D. C. Kilper, P. A. Roos, J. L. Carlsten, and K. L. Lear, Phys. Rev. A **55**, R3323 (1997).
[11] F. Marin, A. Bramati, E. Giacobino, T.-C. Zhang, J.-Ph. Poizat, J.-F. Roch, and P. Grangier, Phys. Rev. Lett. **75**, 4606 (1995).
[12] A. P. Bogatov, P. G. Eliseev, and B. N. Sverdlov, IEEE J. Quantum Electron. **QE-11**, 510 (1975).
[13] H. Ishikawa, M. Yano, and M. Takusagawa, Appl. Phys. Lett. **40**, 553 (1982).
[14] G. P. Agrawal, J. Opt. Soc. Am. B **5**, 147 (1988).
[15] C. B. Su, J. Schlafer, and R. B. Lauer, Appl. Phys. Lett. **57**, 849 (1990).
[16] C. Becher and K.-J. Boller, Opt. Commun. **147**, 366 (1998).
[17] J. Manning, R. Olshansky, D. M. Fye, and W. Powazinik, Electron. Lett. **21**, 496 (1985).
[18] K. Y. Lau and H. Blauvelt, Appl. Phys. Lett. **52**, 694 (1988).
[19] G. P. Agrawal, IEEE J. Quantum Electron. **QE-23**, 860 (1987).
[20] M. Sargent III, S. W. Koch, and W. W. Chow, J. Opt. Soc. Am. B **9**, 1288 (1992).
[21] X. Lu, C. B. Su, R. B. Lauer, G. J. Meslener, and L. W. Ulbricht, J. Lightwave Technol. **12**, 1159 (1992).
[22] O. Hess, S. W. Koch, and J. V. Moloney, IEEE J. Quantum Electron. **31**, 35 (1995).
[23] O. Hess and T. Kuhn, Phys. Rev. A **54**, 3347 (1996).
[24] A. Stahl and I. Balslev, *Electrodynamics of the Semiconductor Band Edge* (Springer-Verlag, Berlin, 1987).
[25] S. Kasapi, S. Lathi, and Y. Yamamoto, Opt. Lett. **22**, 478 (1997).
[26] F. Marin, A. Bramati, V. Jost, and E. Giacobino, Opt. Commun. **140**, 146 (1997).
[27] K.-J. Boller, M. Scheidt, B. Beier, C. Becher, M. E. Klein, and D. H. Lee, Quantum Semiclassic. Opt. **9**, 173 (1997).